PAMAM dendrimer-enhanced DNA biosensors based on electrochemical impedance spectroscopy

Ningning Zhu,*[a] Huan Gao,[a] Yunfeng Gu,[a] Qin Xu,[a] Pingang He[b] and Yuzhi Fang*[b]

Received 5th September 2008, Accepted 3rd February 2009
First published as an Advance Article on the web 23rd February 2009
DOI: 10.1039/b815488k

A novel, simple and sensitive DNA biosensor based on DNA–poly(amidoamine) (PAMAM) dendrimer nanoconjugates was developed by using the electrochemical impedance spectroscopy (EIS) technique. In this context, the assay relies on the hybridization of the single-stranded DNA (ssDNA) probe covalently conjugated on a mercaptoacetic acid self-assembled monolayer on gold electrodes, with the generation 4.5 (G-4.5) PAMAM–target DNA complex in solution. Once the double-stranded DNA (dsDNA) formed on the gold electrodes, G-4.5 PAMAM bearing carboxyls on the periphery was anchored on the hybrids; the changes of interfacial electron-transfer resistance (R_{et}) of the electrodes were measured using an $Fe(CN)_6^{3-/4-}$ redox probe by electrochemical impedance spectroscopy. The results showed that only a complementary sequence could form a dsDNA–PAMAM with the DNA–PAMAM probe and give an obviously enlarged R_{et} value. The non-complementary and three-base mismatched sequence exhibited negligible impedance change compared with the blank measurement (the blank measurement means: ssDNA probe-modified gold electrode was directly measured by EIS). The unique spherical structure combining with more negative charges on the G-4.5 PAMAM periphery anchored on the hybrids could significantly amplify the hybridization signal (R_{et} value), and the detection limit for measuring the full complementary sequence is down to pM level.

Introduction

The sensitive detection of specific DNA sequences is of great significance for a variety of applications, including DNA diagnostics, gene analysis, fast detection of biological warfare agents, and forensic applications.[1–3] Detection of genetic mutations at the molecular level opens up the possibility of performing reliable diagnostics even before any symptom of a disease appears.[2] DNA biosensors (also called genosensors) exploit the preferential binding of complementary single-stranded DNA sequences; the system usually relies on the immobilization of a single-stranded DNA (ssDNA) probe onto a surface to recognize its complementary DNA target sequence by hybridization. Various techniques including fluorescence,[4–6] surface plasmon resonance,[7,8] optical,[9] and electrochemical methods[10] have been used for DNA hybridization detection. Among all these developed technologies, electrochemical techniques[11,12] possess the advantages of being simple design, low cost, of small dimensions and sensitive. One typical example concerning electrochemical DNA sensors involves the assembly of single-stranded DNA probes on the electrode surface followed by hybridization with the complementary target strands. The electrochemical readout is based on using redox reactions or labels[13,14] which trigger an electrochemical signal upon the hybridization of the complementary DNA (cDNA) strand;[10c] this can be easily achieved by intercalating redox species[15,16a] in the double-stranded DNA (dsDNA) or by labeling the complementary target with an electroactive species. For example, Moller *et al.* demonstrated a scheme for DNA detection based on conjugated gold nanoparticles, in which silver was applied to enhance their conductivity, and achieving a high sensitivity.[14f] Hansen *et al.* described a method to detect DNA at the femtomolar level by using the anodic stripping voltammetry of metal sulfide nanoparticles.[14g] Wang *et al.* presented an electrochemical hybridization assay based on quantum dot nanocrystals.[14c]

The biosensor based on direct electrical measurement has also attracted more and more attention.[12] The directly measured parameters include resistance,[12a] impedance, capacitance, *etc.* Some label-free electrochemical DNA biosensors by electrochemical impedance spectroscopy (EIS) have also been reported.[17] For example, Li *et al.*[17e] and Lee and Shim[17f] have reported label-free DNA hybridization detection based on impedance spectroscopy. Yang and co-workers[17g] reported a dendrimer-modified electrode to prepare DNA biosensor impedance. Kraatz and co-workers have detected mismatched single-nucleotide with the microarray electrode.[17h] A DNA probe grafted onto a conducting polythiophene film[18a] or a copolymer of poly-[pyrrole-*co*-4-(3-pyrrolyl)butanoic acid][18b] was used to hybridize with single-stranded complementary target, and EIS was used to probe the conducting properties or charge-transfer resistance of the film changed upon hybridization. A DNA probe was also covalently immobilized on a quinone-containing polymer; after hybridization, the electrochemical impedance spectra and CVs were obtained due to changes in the conformation on the polymeric film.[18c] Korri-Youssoufi and co-workers developed an electrochemical biosensor based on a precursor polymer bearing an ester group on which amino-DNAs were directly immobilized

[a]*Department of Chemistry, Shanghai Normal University, Shanghai 200234, China. E-mail: zhunn@shnu.edu.cn*
[b]*Department of Chemistry, East China Normal University, Shanghai 200062, China*

by substitution. In the presence of the complementary sequence, a significant change in the voltammogram was observed by CV due to the occurrence of a hybridization event.[18d,e] The terthiophene polymer containing a carboxyl group on a GCE was used to covalently graft a DNA probe, where the impedance and admittance changes were obtained before and after hybridization.[18f]

Poly(amidoamine) (PAMAM) dendrimers, as well as other families of dendrimers, are three-dimensional nanosized synthetic molecules that have internal cavities and numerous surface groups, possessing the advantages of non-toxic, biocompatible, adequate functional groups for chemical fixation, limited body accumulation, and which enable them to be used as a synthetic vector for the delivery of genes.[19] Recently, increasing attention has been received in sensing applications. The amine- or carboxyl-terminated dendrimers on their periphery have the advantages of being able to be conjugated to other molecules *via* an amide linkage, which is one of the most fundamental and widespread chemical bonds in nature. For instance, the amine-terminated PAMAM dendrimers were attached to an activated mercaptoundecanoic acid (MUA) self-assembled monolayer (SAM) *via* covalent amide linkages.[20]

In this article, a carboxyl-terminated generation 4.5 (G-4.5) PAMAM dendrimer with a trimesyl core, a new class of nanoscopic, spherical polymers, was covalently conjugated with the amino group-modified target ssDNA at the 5′-end,[21] the so-called PAMAM–DNA target. Once the hybridization events happen between the ssDNA probe immobilized on the gold electrode and the PAMAM–DNA target in solution, the change of electrode interfacial properties was measured by EIS (as shown in Scheme 1). Compared with the dsDNA without the PAMAM label, the dsDNA with PAMAM tags yielded more resistance for electron transfer from solutions to the electrode surface because of the more negative charges and space resistance of G-4.5 PAMAM; and as a result, an improved sensitivity over 2 orders of magnitude for sequence-specific DNA detection was obtained.

Experimental

Chemicals and solutions

24-base synthetic oligonucleotides were purchased from Shenggong Bioengineering Ltd Company (Shanghai, China); probe sequence: 5′-NH_2-GAG CGG CGC AAC ATT TCA GGT CGA-3′; the fully complementary target sequence: 5′-NH_2-TCG ACC TGA AAT GTT GCG CCG CTC-3′ (T_m: 75 °C); a three-base mismatch oligonucleotide sequence: 5′-NH_2-TCG ***T***CC TGA AA***C*** GTT GCG CC***T*** CTC-3′ (T_m: 68 °C); the non-complementary oligonucleotide sequence: 5′-NH_2-GAG CGG CGC AAC ATT TCA GGT CGA-3′ (the same as the probe sequence without the amino-group attachment at the 5′-end). 1-Ethyl-3-(3-dimethylaminopropyl)carbodiimide hydrochloride (EDC), mercaptoacetic acid (RSH) (SH–CH_2–COOH) and 2-thioethanol were purchased from Sigma (US). The following buffers were used: 0.1 M PBS (0.1 M NaCl, 0.01 M sodium phosphate buffer, pH 7.0), 0.3 M PBS (0.3 M NaCl, 0.01 M sodium phosphate buffer, pH 7.0) and 0.75 M PBS (0.75 M NaCl, 0.01 M sodium phosphate buffer, pH 7.0). The carboxyl-terminated PAMAM G-4.5 dendrimers with a trimesyl core were obtained from Dr Yang Shiping (Shanghai Normal University). The G-4.5 PAMAM dendrimers were synthesized according to the reported literature.[19d] First, methyl trimesate (1.4 g) was dissolved in 50 mL of methanol and was added dropwise to 75 mL of ethylenediamine in the presence of an ice water bath. Under a nitrogen atmosphere, the mixture was stirred in darkness at room temperature for 72 h. Ethylenediamine was removed by evaporation and then coevaporation after dissolving in the mixture of 10 mL of methanol and 100 mL of toluene. This process was repeated three times. The yellow oil-like G-1 was obtained. Then, G-1 was dissolved in 70 mL of methanol, and 3 mL of methyl acrylate was added dropwise under a nitrogen atmosphere. Sodium methoxide solution was added as a catalyst. The mixture was stirred in darkness at room temperature for 72 h. The solvent and excess methyl acrylate were removed under a vacuum to give a yellow oil-like G-1.5. G-4.5 PAMAM dendrimer was synthesized similarly by repeating the above-mentioned steps through adding ethylenediamine and methyl acrylate in turn. Polymer was characterized by Fourier transform infrared (FT-IR) spectra and ^{1}H NMR, and these will be reported elsewhere. Other reagents were commercially available and were all of analytical reagent grade. All of the solutions were prepared with doubly distilled water.

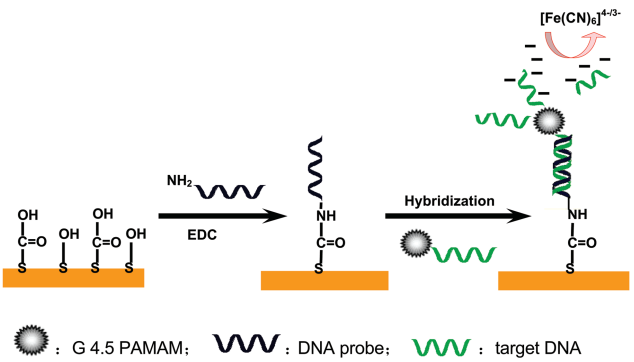

Scheme 1 Schematic representation of ssDNA probe-modified gold electrode hybridized with ssDNA–PAMAM target and the formation of dsDNA–PAMAM hybrid.

Preparation of ssDNA probe-modified gold electrodes

Gold electrodes (2.0 mm in diameter, CHI instruments) were polished with alumina powder (0.3 and 0.05 μm) and sonicated in acetone and doubly distilled water (each for 3–5 min). Then the gold electrode was cleaned with a hot mixture of piranha solution (a 1 : 3 mixture of 30% H_2O_2/conc. H_2SO_4) during 5 min and then washed in doubly distilled water. Cyclic voltammetry (voltage range 0.3–1.5 V vs. SCE, scan rate 0.2 V/s) was applied for final electrochemical cleaning in 0.2 M H_2SO_4 until a cyclic voltammogram characteristic of a clean Au electrode was obtained. The electrode was then washed in doubly distilled water. Chemical modification of the clean Au electrodes was carried out by exposing the substrate to a 2-thioethanol/RSH mixed solution (3 : 1 ratio) for 2 h to obtain a self-assembled mixed monolayer-modified gold electrode, and then 24-base 5′-NH_2-modified ssDNA probes (2.25 μM) were coupled to the surface in the presence of the coupling reagent EDC and acetate buffer (pH 5.2) for 10 h with stirring at room temperature, as depicted in

Scheme 1. The incorporation of 2-thioethanol in the mixed monolayer was anticipated to prevent non-specific adsorption of the ssDNA probe or others onto the electrode surface. The electrode was washed with acetate buffer (pH 5.2) and water for 5 min each to remove any unbound DNA probe.

Preparation of PAMAM–DNA complex and its hybridization with DNA probe on Au electrodes

The PAMAM–DNA complex was prepared by mixing 3 mL G-4.5 PAMAM solution (2 mg/mL, pH 5.2) with 2 OD (about 66 μg) target ssDNA containing 5 mM EDC with gentle stirring for 12 h at ambient temperature. After that, ethanol and 3 M acetate buffer (pH 5.2) in the ratio of 20 : 1 (V/V) were added and the solution was placed in a refrigerator (<−15 °C) for 20 min. After being centrifuged, the precipitate was washed with 70% ethanol (40 μL × 3) to remove unreacted PAMAM.[22] The obtained precipitate was dispersed in 0.1 M PBS, and the free DNA was separated from the PAMAM–DNA complex using Amicon Y100 molecular weight cutoff filters. The filters and solution were spun at 10 000g for 8 minutes with no more than 300 μL of the DNA–PAMAM solution on the Y100 filter. The majority of the free DNA, oligonucleotide not in conjugation with PAMAM, passes through the filter and the DNA–PAMAM remains on the filter. Thus the free DNA was removed from the PAMAM–DNA complex. The obtained G-4.5 PAMAM–DNA complex was dissolved in water for further DNA hybridization immediately or stored in a refrigerator (−15 °C). Thus ssDNA was attached onto the surface of the G-4.5 PAMAM *via* an amide linkage between the free amino groups of the ssDNA at the 5′-end and the carboxyl of the PAMAM on the periphery.[21]

Hybridization reaction was carried out by immersing the ssDNA probe-captured electrode into a stirred hybridization solution (0.3 M PBS buffer, pH 7.0) containing a certain concentration of DNA target (the full complementary target; a three-base mismatched oligonucleotide and a non-complementary sequence) for 60 min at 37 °C. After that, the electrode was rinsed three times with 0.75 M phosphate buffer (0.75 M NaCl, pH 7.0) and water respectively, to remove the non-hybridized physically adsorbed target DNA.

Instruments and measurements

AC impedance (ACI) measurements and cyclic voltammetry (CV) scans were all performed with a CH Instruments Model 660B electrochemical analyzer (CH Instruments Inc., US). The three-electrode system consisted of a gold working electrode (CH Instruments, US), a saturated calomel electrode (SCE) reference electrode (saturated KCl), and a platinum wire counter electrode. All electrochemical measurements were carried out in a 10 mL cell.

Atomic force microscope (AFM) experiments were performed with a Veeco Nano III (USA) scanning probe microscope operated in tapping mode under ambient conditions. Ultrathin films of G-4.5 PAMAM were prepared by spin-coating a solution of known concentration on freshly cleaved mica surfaces, which were then air-dried at room temperature. Silicon tapping probes having a spring constant of *ca.* 30 N/m with about 5–10 nm radius were used for tapping scans. Image analysis was performed with TopoMetrix SPMLab 3.06.06 software. UV-Vis spectra were recorded with a Varian Cary 50 UV-Vis spectrophotometer (US).

Faradaic impedance measurements were performed in a 0.1 M PBS buffer solution (pH 7.0) containing a 1 mM $K_3[Fe(CN)_6]$/$K_4[Fe(CN)_6]$ (1 : 1) mixture as a redox probe. Impedance measurements were performed at a bias potential of 0.19 V (vs. SCE) in the frequency range from 10^5 Hz to 1.0 Hz at a sampling rate of 12 points per decade (AC amplitude: 5 mV). The impedance spectra were plotted in the form of complex plane diagrams (Nyquist plots, Z_{im} vs. Z_{re}). All the electrochemical measurements were performed at ambient temperature.

Results and discussion

Faradaic impedance spectroscopy (EIS) is an effective technique to probe the features of surface-modified electrodes.[23] The impedance data were fitted with commercial software Zview2. A modified Randle's equivalent circuit and the fitting of one measured spectrum to the equivalent circuit are shown in Fig. 1.[16b] The circuit, which is often used to model interfacial phenomena, included the following: R_s, the ohmic resistance of the electrolyte solution; Z_w, the Warburg impedance, resulting from the diffusion of ions from the bulk electrolyte to the electrode interface; C_{dl}, the interfacial double layer capacitance between an electrode and a solution; R_{et}, corresponding to the interfacial electron-transfer resistance for the redox prober. The parallel elements (CPE and Z_w + R_{et}) of the equivalent circuit were introduced since the total current through the working interface was the sum of respective contributions from the Faradaic process and the double layer charging. The impedance spectra include a semicircle portion and a linear portion. The semicircle portion at higher frequencies corresponds to the electron-transfer-limited process, and the linear portion at lower frequencies represents the diffusion-limited process. The semicircle diameter equals the electron-transfer resistance R_{et}. Here R_{et} was a suitable signal for sensing the interfacial properties of the prepared biosensors.

PAMAM dendrimers have a monodispersed spherical conformation with a highly branched three-dimensional

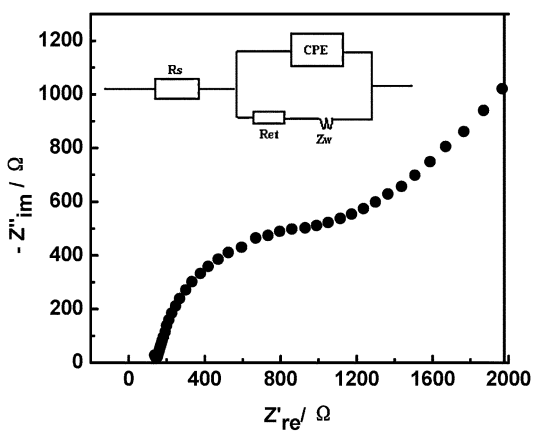

Fig. 1 Faradaic impedance spectra presented in the form of a Nyquist plot, Z_{im} vs. Z_{re}, in the presence of the redox probe. Inset: equivalent circuit corresponding to the impedance features.

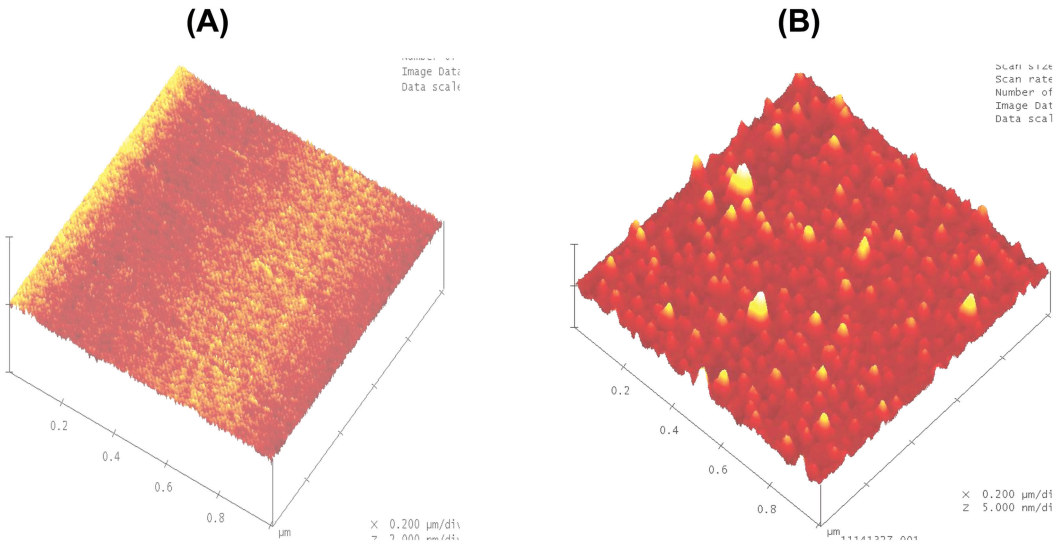

Fig. 2 Atomic force microscope (AFM) images of PAMAM dendrimers. (A): AFM image of bare mica surface; (B): AFM image of PAMAM (G-4.5, 0.2%) on the mica surface.

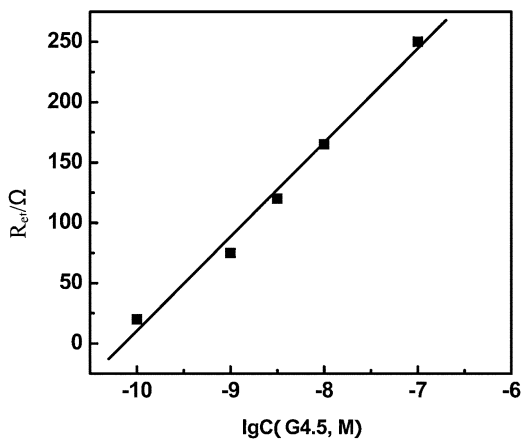

Fig. 3 Diagrams of electron-transfer resistance (R_{et}) corresponding to different concentrations of G-4.5 PAMAM.

structure that provides a scaffold for the attachment of multiple biomolecules. Atomic force microscope images of generation 4.5 PAMAM with a trimesyl core (0.2%, w/w) are shown in Fig. 2. It demonstrates the shape and consistency of the PAMAM molecules. To investigate the effect of the carboxyl-terminated G-4.5 PAMAM dendrimer on the interfacial electron-transfer resistance on gold electrodes, a series of different concentrations of G-4.5 PAMAM solutions were cast on the gold electrodes for a certain time, then Faradaic impedance measurements were preformed in a 0.1 M PBS buffer solution (pH 7.0) containing a 1 mM $K_3[Fe(CN)_6]/K_4[Fe(CN)_6]$ (1 : 1) mixture. As shown in Fig. 3, the electron-transfer resistance (R_{et}) increased with the increase of G-4.5 PAMAM concentration on the gold electrodes from 10^{-10} to 10^{-7} M. It was concluded that a low concentration of G-4.5 PAMAM could effectively increase the R_{et} value of $K_3[Fe(CN)_6]/K_4[Fe(CN)_6]$ from the solution to the electrode surface, owing to the electrostatic repulsion between the negatively charged $Fe(CN)_6^{3-/4-}$ probe and the carboxyl-terminated G-4.5 PAMAM dendrimer attached on the electrode. So we choose G-4.5 PAMAM as a signal amplification tag for further DNA hybridization detection.

Fig. 4 shows the UV-Vis spectrum of the PAMAM–DNA target conjugation measured by the Varian Cary 50 UV-Vis spectrophotometer using the bare PAMAM as a blank. As can be seen, an absorption band appeared at *ca.* 277 nm, which corresponded to the characteristic absorption of DNA base. The 17 nm-shift of the adsorption peak from 260 to 277 nm may be due to the interaction between PAMAM and DNA, suggesting that the DNA molecules were successfully conjugated onto the G-4.5 PAMAM. As a control, the adsorption spectra of ssDNA and PAMAM solution before the conjugation reaction were also measured by the Varian Cary 50 UV-Vis spectrophotometer. As expected, DNA solution shows an adsorption band at *ca.* 260 nm, which is attributed to the characteristic adsorption of DNA base; while PAMAM solution exhibited a strong and another moderate adsorption peak at 225 and 290 nm, respectively, which corresponded to the adsorption peak of the benzene ring in G-4.5 PAMAM. To verify that the covalent bond formation between

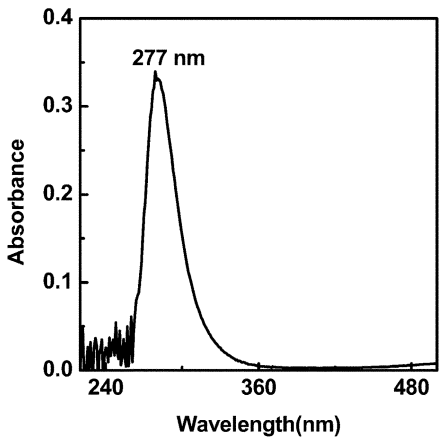

Fig. 4 UV-Vis spectrum of the PAMAM–DNA target conjugation using the bare PAMAM solutions as the blank.

the G-4.5 PAMAM dendrimer and ssDNA actually takes place, control experiments were performed in which the PAMAM dendrimers were incubated as mentioned above but without adding the coupling agent EDC, then the hybridization reaction and EIS measurement were performed according to the described procedure. Under these conditions, the R_{et} value of the captured DNA probe hybridized with the target DNA–PAMAM mixture in the absence of EDC was equal to that hybridized with target DNA without PAMAM-labeling. It demonstrates that the DNA–PAMAM mixture was unstable in the high salts hybridization buffer solution. On the other hand, an obviously amplified signal was obtained when incubating PAMAM and ssDNA in the presence of EDC. So covalent bond formation takes place between the PAMAM dendrimer molecules and ssDNA oligonucleotides.

The stepwise electrode modification process was studied with EIS, as displayed in Fig. 5. At the bare Au electrode, a small electron-transfer resistance (R_{et}) was recorded, suggesting a fast electron-transfer process at such an electrode (black ■). Compared with the bare Au electrode, the self-assembled monolayer-modified Au electrode shows a larger R_{et} (green ▲), mainly due to the enlarged charge-transfer distance caused by the electrostatic repulsion between the $Fe(CN)_6^{3-/4-}$ redox couple and the negatively charged $-COO^-$ groups assembled on the Au electrode. After activation by EDC, R_{et} decreased significantly, even lower than for the bare Au electrode (red ◆). This can be explained in that the negative charges of the $-COO^-$ groups were sealed, and the net positive charge adduct carrying under the experimental conditions would attract the negative redox probe. The R_{et} increased after the ssDNA was immobilized on the electrode surface (magenta ○), and we reasoned this as the fact of the electrostatic repulsion interaction between the negatively charged DNA backbone and the $Fe(CN)_6^{3-/4-}$ redox couple.

The hybridization efficiency has been found to depend on the second structure of the probe, as well as on the distribution of the probe on the substrate.[24a] The DNA surface density was

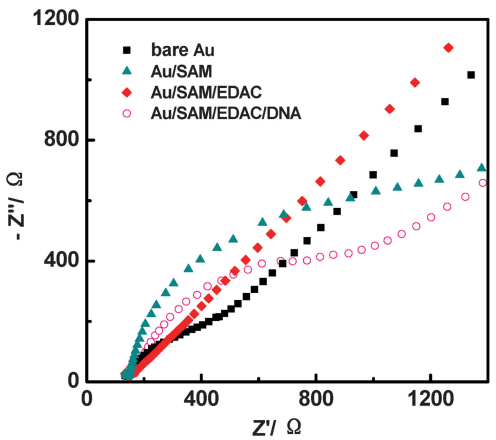

Fig. 5 Faradaic impedance spectra obtained in the 0.1 M PBS buffer solution containing a 1 mM $K_3[Fe(CN)_6]/K_4[Fe(CN)_6]$ (1 : 1) mixture at a potential of 0.19 V (vs. SCE) in the frequency for 100 000 Hz to 1 Hz, a sampling rate of 12 points per decade, AC amplitude 5 mV. The bare gold electrode (■), carboxyl-terminated SAM-modified Au electrode (▲), EDC activated SAM-functionalized Au electrode (◆), ssDNA-containing SAM-functionalized Au electrode (○).

determined using a chronocoulometric method based on that reported by Steel *et al.*[24b] The DNA-functionalized electrode was first immersed in a low ionic strength electrolyte, 10 mM Tris–HCl buffer pH 7.4, the potential stepped from +150 mV to −450 mV vs. Ag/AgCl with a pulse period of 500 ms, and the resulting charge flow measured. The electrode was then immersed in a solution of 100 μM hexaammineruthenium(III) chloride $[Ru(NH_3)_6]^{3+}$ in Tris–HCl buffer, and the measurement was repeated. Both solutions were purged with nitrogen for at least 30 min prior to the experiment, and blanketed with nitrogen during the experiment. The surface coverage of $[Ru(NH_3)_6]^{3+}$ was calculated as the difference in the chronocoulometric intercepts in the absence and presence of $[Ru(NH_3)_6]^{3+}$. The surface coverage of the $[Ru(NH_3)_6]^{3+}$ is then converted to DNA surface density with the relationship $C_{DNA} = C_0(z/m)$, where C_{DNA} = the surface density of DNA, C_0 = the surface coverage of $[Ru(NH_3)_6]^{3+}$, z = the charge of $[Ru(NH_3)_6]^{3+}$ and m = the number of bases of DNA. A surface coverage of $1.8 \times 10^{12}/cm^2$ DNA probe was estimated from the Cottrell's experiment with $[Ru(NH_3)_6]^{3+}$ in a weak electrolyte,[24b,c] which is beneficial for improving the detection sensitivity because of the probe densities in the range $(1–3) \times 10^{12}/cm^2$ are often of most interest for DNA biosensors due to the high surface density of hybridized target that is obtained.[24b]

Fig. 6A illustrated an R_{et} increase corresponding to the ssDNA-modified electrode before (■) and after incubating with the same concentration (1.0×10^{-10} M) of the complementary PAMAM–target sequence (●) and the complementary target without PAMAM tags (▲). We can see that the electron-transfer resistance R_{et} was obviously enlarged after hybridization with the complementary PAMAM–target sequence compared with that of the complementary target sequence without PAMAM tags. Probe-modified electrodes were also tested with different concentrations of complementary target–PAMAM complex. It was exhibited that, with the increase of complementary target concentration, greater changes in electrochemical impedance spectra were observed. Thus, the proposed electrochemical sensor can be used for the quantitative detection of specific DNA sequences. It was shown that the analytical signal, ΔR_{et} ($R_{et,dsDNA} - R_{et,ssDNA}$), had a linear relationship with the logarithmic value of the complementary target DNA–PAMAM concentration ranging from 10^{-11} to 10^{-8} M (Fig. 6B, black ■). The regression equation was $\Delta R_{et} = 3405.7 + 306.4 \log C_{target}$ with a correlation coefficient (R) of 0.9953. The detection limit was 2.5×10^{-12} M using $3s$ (where s is the standard deviation of the blank solution, $n = 11$). As a control, when probe-modified electrodes were incubated with the same concentration of target ssDNA without PAMAM tags, a smaller increase of the electron-transfer resistance was obtained (Fig. 6A, ▲); the regression equation was $\Delta R_{et} = 1615.6 + 153.6 \log C_{target}$ (Fig. 6B, red ●) with a correlation coefficient (R) of 0.9849; the detection limit was 1.5×10^{-10} M. The results show that the target DNA–PAMAM conjugation could significantly enhance the hybridization signal, and a decreased 2 orders of magnitude detection limit was obtained for complementary sequence detection relative to that without PAMAM conjugation. This protocol eliminated the complex electrochemical detection process compared with the reported stripping voltammetry.[25a–c] The sensitivity of the method is superior to the recently reported polymer film-based label-free

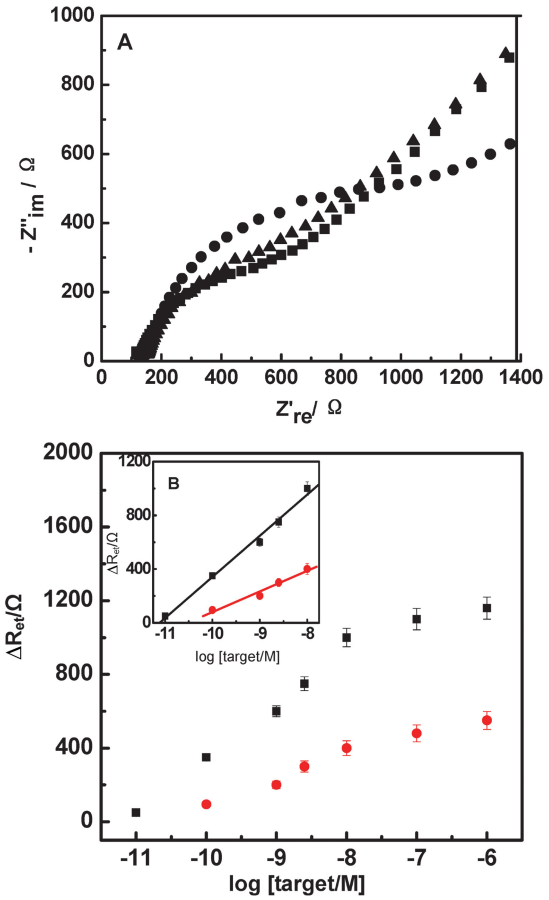

Fig. 6 (A) Faradaic impedence spectra that corresponding to the ssDNA-modified electrode before (■) and after incubating with the same concentration (1.0×10^{-10} M) of the complementary PAMAM–target sequence (●) and the complementary target without PAMAM tags (▲) in PBS (10 mM, pH 7.4) solution containing 0.1 M KCl and 1 mM $Fe(CN)_6^{3-/4-}$. (B) The plots of ΔR_{et} vs. complementary target concentration, hybridized with the complementary target with PAMAM tags (black ■) and without PAMAM tags (red ●) at 37 °C with 60 min stirring.

biosensors with a detection limit of 0.5 nM[25d] and 20 nM[25e] by EIS. Although the detection limit of the present method is inferior to that (0.01 pM) based on enzyme-amplified electronic transduction of single-base DNA mutations,[25f] it is competitive with the reported negatively charged liposomes as tags to amplify DNA sensing processes (detection limit: pM).[25g]

The selectivity of the PAMAM–target complex-based electrochemical hybridization assay was investigated by using the same concentration (1.0×10^{-9} M) of the oligonucleotide DNA target–PAMAM complex, including the complete complementary, a non-complementary and a three-base mismatched sequence, to hybridize with the probe ssDNA immobilized on the gold electrode. It was observed that only the full complementary sequence gave a significant response; the non-complementary and a three-base mismatched sequence had a slight change in R_{et} compared with that of the ssDNA-modified electrode (shown in Fig. 7), indicating that the DNA biosensor had a good selectivity. On the other hand, to eliminate the influence of non-conjugated PAMAM on the electrochemical impedance signal, the control

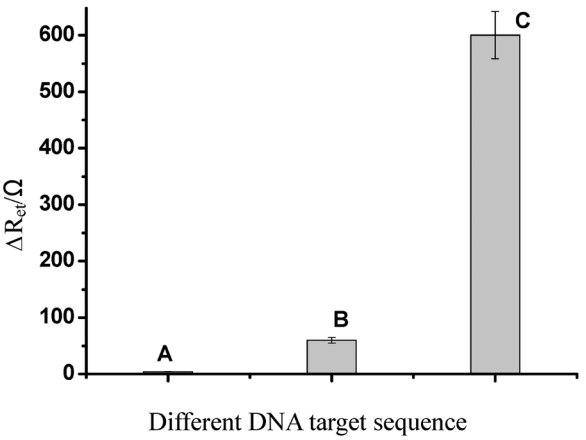

Fig. 7 The ΔR_{et} corresponding to ssDNA probe-containing electrode incubating with the same concentration (1.0×10^{-9} M) of different PAMAM–ssDNA target (A: the non-complementary sequence; B: a three-base mismatched sequence and C: the complementary sequence) at 37 °C for 60 min with gentle stirring.

experiments were performed as follows: the DNA probe-modified Au electrode was incubated with the full complementary DNA target–PAMAM complex and bare G-4.5 PAMAM solution for a certain time, respectively, and then the electrochemical impedance measures were conducted according to the described procedure. It was found that the impedance signals of the probe-modified electrode have an obvious increase after incubating with the complementary DNA target–PAMAM complex, but no obvious change occurred after incubating in bare PAMAM (figure not shown), further showing that the described sensors have no non-specific adsorption.

Several relevant experimental parameters playing an important effect on the impedance signal change, including the RSH self-assembly extent and the solution ionic strength for EIS detection, were all investigated here. Various thioalkanes and thioalcohols[26a–c] have been used for creating a mixed monolayer to control the surface density of the probes, which is a crucial parameter in the design of a sensitive and selective sensor.[26d,e] In this article, a 2-thioethanol/RSH mixed monolayer (3 : 1 ratio) was used to assemble on an Au electrode, and then 5′-NH_2-modified DNA probes were coupled to the surface in the presence of EDC. Here thioalcohols were used as interstitial spacers in mixed SAMs to reduce non-specific absorption of the DNA probes to the gold and also to control the probe density on the electrode. Moreover, in order to ensure a moderate monolayer film for an ideal signal change, a 2-thioethanol/RSH mixed solution (3 : 1 ratio) for a 2 h assembly time was applied. The ionic strength of the background electrolyte also affected the impedance signal change. It was found that, at a lower ionic strength (10 mM phosphate buffer + 0.01 M NaCl, pH 7.0), a higher ΔR_{et}-to-$R_{et,ssDNA}$ (signal-to-background) was obtained; and the concentration of NaCl in the phosphate buffer showed a more obvious effect on the impedance change than that of phosphate buffer. Therefore, if the background electrolyte ionic strength is lowered, an increased signal-to-background could be obtained. However, giving attention to the stability of the dsDNA, a 0.1 M PBS (0.1 M NaCl + 10 mM sodium phosphate buffer, pH 7.0) was chosen as the detection electrolyte.

Conclusions

In summary, we described a new, sensitive DNA biosensor based upon PAMAM enlargement by EIS measurements. Due to the unique properties of PAMAM dendrimers and abundant negative charges on the periphery of the PAMAM, the detection signal of the DNA biosensor was obviously enhanced, and the sensitivity of the method was effectively improved.

Acknowledgements

We gratefully acknowledge the financial support from NSF of China (Grant Numbers 20705020), China Postdoctoral Science Foundation and Shanghai Leading Academic Discipline Project (T0402 and 07dz22303).

References

1 J. Wang, *Nucleic Acids Res.*, 2000, **28**, 3011.
2 A. Sassolas, B. Leca-Bouvier and L. Blum, *Chem. Rev.*, 2008, **108**, 109.
3 N. Schork, D. Fallin and J. Lanchbury, *Clin. Genet.*, 2000, **58**, 250.
4 D. Gerion, W. Parak, S. Williams, D. Zanchet, C. Micheel and A. Alivisatos, *J. Am. Chem. Soc.*, 2002, **124**, 7070.
5 M. Bruchez, M. Moronne, P. Gin, S. Weiss and A. Alivisatos, *Science*, 1998, **281**, 2013.
6 W. Chan and S. Nie, *Science*, 1998, **281**, 2016.
7 L. He, M. Musick, S. Nicewarner, F. Salinas, S. Benkovic, M. Natan and C. Keating, *J. Am. Chem. Soc.*, 2000, **122**, 9071.
8 B. Nelson, T. Grimsrud, M. Liles, R. Goodman and R. Corn, *Anal. Chem.*, 2001, **73**, 1.
9 (*a*) N. Rosi and C. Mirkin, *Chem. Rev.*, 2005, **105**, 1547; (*b*) R. Elghanian, J. Storhoff, R. Mucic, R. Letsinger and C. Mirkin, *Science*, 1997, **277**, 1078.
10 (*a*) C. Yu, Y. Wan, H. Yowanto, J. Li, C. Tao, M. James, C. Tan, G. Balckburn and T. Meade, *J. Am. Chem. Soc.*, 2001, **123**, 11155; (*b*) J. Wang, D. Xu, A. Kawde and R. Polsky, *Anal. Chem.*, 2001, **73**, 5576; (*c*) T. Drummond, M. Hill and J. Barton, *Nat. Biotechnol.*, 2003, **21**, 1192; (*d*) Y. Xiao, A. Lubin, B. Baker, K. Plaxco and A. Heeger, *Proc. Natl. Acad. Sci. USA*, 2006, **103**, 16677; (*e*) K. Odenthal and J. Gooding, *Analyst*, 2007, **132**, 603; (*f*) S. Pinijsuwan, P. Rijiravanich, M. Somasundrum and W. Surareungchai, *Anal. Chem.*, 2008, **80**, 6779.
11 (*a*) E. Palecek and M. Fojta, Electrochemical DNA Sensors, in *Bioelectronics: From Theory to Applications*, ed. I. Willner and E. Katz, Wiley-VCH, Weinheim 2005, pp. 127–192; (*b*) *Electrochemistry of Nucleic Acids and Proteins. Towards Electrochemical Sensors for Genomics and Proteomics*, ed. E. Palecek, F. Scheller and J. Wang, Elsevier, Amsterdam 2005; (*c*) C. Thaxton, H. Hill, D. Georganopoulou, S. Stoeva and C. Mirkin, *Anal. Chem.*, 2005, **77**, 8174; (*d*) J. Nam, S. Stoeva and C. Mirkin, *J. Am. Chem. Soc.*, 2004, **126**, 5932; (*e*) Y. Fan, X. Chen, C. Tung, J. Kong and Z. Gao, *J. Am. Chem. Soc.*, 2007, **129**, 5437.
12 (*a*) S. Park, T. Taton and C. Mirkin, *Science*, 2002, **295**, 1503; (*b*) E. Braun, Y. Eichen, U. Sivan and G. Ben-Yoseph, *Nature*, 1998, **391**, 775.
13 (*a*) T. Livache, A. Roget, E. Dejean, C. Barthet, G. Bidan and R. Teoule, *Nucleic Acids Res.*, 1994, **22**, 2915; (*b*) T. Lumley, C. Campbell and A. Heller, *J. Am. Chem. Soc.*, 1996, **118**, 5504.
14 (*a*) J. Wang, D. Xu, A. Kawde and R. Polsky, *Anal. Chem.*, 2001, **73**, 5576; (*b*) L. Authier, C. Grossiord, P. Brossier and B. Limoges, *Anal. Chem.*, 2001, **73**, 4450; (*c*) J. Wang, G. Liu and A. Merkoci, *J. Am. Chem. Soc.*, 2003, **125**, 3214; (*d*) J. Wang, G. Liu and Q. Zhu, *Anal. Chem.*, 2003, **75**, 6218; (*e*) I. Willner and E. Katz, *Angew. Chem., Int. Ed.*, 2004, **43**, 6042; (*f*) R. Moller, A. Csaki, J. Kohler and W. Fritzsche, *Langmuir*, 2001, **17**, 5426; (*g*) J. Hansen, R. Mukhopadhyay, J. Hansen and K. Gothelf, *J. Am. Chem. Soc.*, 2006, **128**, 3860.
15 (*a*) J. Wang, J. Fernandes and L. Kubota, *Anal. Chem.*, 1998, **70**, 3699; (*b*) J. Liu, S. Tian, L. Tiefenauer, P. Nielsen and W. Knoll, *Anal. Chem.*, 2005, **77**, 2756.
16 (*a*) G. Marrazza, G. Chiti, M. Mascini and M. Anichini, *Clinical Chemistry*, 2000, **46**, 31; (*b*) A. Bard and L. Faulkner, *Electrochemical Methods: Fundamentals and Applications*, 2nd edn, Wiley, New York, 2001.
17 (*a*) E. Souteyrand, J. Cloarec, J. Martin, C. Wilson, I. Lawrence, S. Mikkelsen and M. Lawrence, *J. Phys. Chem. B*, 1997, **101**, 2980; (*b*) Y. Fu, R. Yuan, L. Xu, Y. Chai, Y. Liu, D. Tang and Y. Zhang, *Biochem. Biophys. Methods*, 2005, **62**, 163; (*c*) M. Vagin, S. Trashin, A. Karyakin and M. Mascini, *Anal. Chem.*, 2008, **80**, 1336; (*d*) H. Peng, C. Soeller and J. Travas-Sejdic, *Macromolecules*, 2007, **40**, 909; (*e*) C. Li, C. Sun, S. Song, V. Choong, G. Maracas and X. Zhang, *Front. Biosci.*, 2005, **10**, 180; (*f*) T. Lee and Y. Shim, *Anal. Chem.*, 2001, **73**, 5629; (*g*) A. Li, F. Fang, Y. Ma and X. Yang, *Biosens. Bioelectron.*, 2007, **22**, 1716; (*h*) X. Li, J. Lee and H. Kraatz, *Anal. Chem.*, 2006, **78**, 6096.
18 (*a*) C. Gautier, C. Cougnon, J. Pilard and N. Casse, *Electroanal. Chem.*, 2006, **587**, 276; (*b*) J. Travas-Sejdic, H. Peng, P. Kilmartin, M. Cannell, G. Bowmaker, R. Cooney and C. Soeller, *Synth. Met.*, 2005, **152**, 37; (*c*) B. Piro, J. Haccoun, M. Pham, L. Tran, A. Rubin, H. Perrot and C. Gabrielli, *J. Electroanal. Chem.*, 2005, **577**, 155; (*d*) H. Korri-Youssoufi and A. Yassar, *Biomacromolecules*, 2001, **2**, 58; (*e*) F. Garnier, H. Korri-Youssoufi, P. Srivastava, B. Mandrand and T. Delair, *Synth. Met.*, 1999, **100**, 89; (*f*) T. Lee and Y. Shim, *Anal. Chem.*, 2001, **73**, 5629.
19 (*a*) G. Newkome, C. Moorefield and F. Vögtle, *Dendrimers and Dendrons: Concepts, Syntheses, Applications*, Wiley-VCH, Weinheim, 2002; (*b*) A. Bosman, H. Janssen and E. Meijer, *Chem. Rev.*, 1999, **99**, 1665; (*c*) S. Grayson and J. Frechet, *Chem. Rev.*, 2001, **101**, 3819; (*d*) X. Zhang, X. Wang, S. Huang, R. Zhuo, Z. Liu, H. Mao and K. Leong, *Biomacromolecules*, 2005, **6**, 341.
20 (*a*) M. Wells and R. Crooks, *J. Am. Chem. Soc.*, 1996, **118**, 3988; (*b*) H. Tokuhisa and R. Crooks, *Langmuir*, 1997, **13**, 5608; (*c*) E. Bustos, J. Manriquez, G. Orozco and L. Godinez, *Langmuir*, 2005, **21**, 3013.
21 G. Hermanson, *Bioconjugate Techniques*, Academic Press, New York, 1996.
22 A. Forster, J. McInnes, C. Skingle and H. Symons, *Nucleic Acids Res.*, 1985, **13**, 745.
23 (*a*) X. Ren and P. Pichup, *J. Electroanal. Chem.*, 1997, **420**, 251; (*b*) F. Patoslky, B. Filanovsky, E. Katz and I. Willner, *J. Phys. Chem. B*, 1998, **102**, 10359; (*c*) I. Kowino and O. Sadik, *Electroanalysis*, 2005, **23**, 2101; (*d*) J. Daniels and N. Pourmanda, *Electroanalysis*, 2007, **12**, 1239.
24 (*a*) H. Du, C. Strohsahl, J. Camera, B. Miller and T. Krass, *J. Am. Chem. Soc.*, 2005, **127**, 7932; (*b*) A. Steel, T. Herne and M. Tarlov, *Anal. Chem.*, 1998, **70**, 4670; (*c*) E. Wong and J. Gooding, *J. Am. Chem. Soc.*, 2007, **129**, 8950.
25 (*a*) J. Wang, D. Xu, A. Kawde and R. Polsky, *Anal. Chem.*, 2001, **73**, 5576; (*b*) J. Wang, G. Liu, M. Rasul Jan and Q. Zhu, *Electrochem. Commun.*, 2003, **5**, 1000; (*c*) J. Wang, G. Liu and A. Merkoci, *J. Am. Chem. Soc.*, 2003, **125**, 3214; (*d*) H. Peng, C. Soeller and J. Sejdic, *Macromolecules*, 2007, **40**, 909; (*e*) H. Gu, X. Su and K. Loh, *J. Phys. Chem. B*, 2005, **109**, 13611; (*f*) F. Patolsky, A. Lichtenstein and I. Willner, *Nat. Biotechnol.*, 2001, **19**, 253; (*g*) F. Patolsky, A. Lichtenstein and I. Willner, *J. Am. Chem. Soc.*, 2001, **123**, 5194.
26 (*a*) S. Pan and L. Rothberg, *Langmuir*, 2005, **21**, 1022; (*b*) R. Lao, S. Song, H. Wu, L. Wang, Z. Zhang, L. He and C. Fan, *Anal. Chem.*, 2005, **77**, 6475; (*c*) C. Fan, K. Plaxco and A. Heeger, *Proc. Natl. Acad. Sci. USA*, 2003, **100**, 9134; (*d*) H. Du, M. Disney, B. Miller and T. Krauss, *J. Am. Chem. Soc.*, 2003, **125**, 4012; (*e*) H. Du, C. Strohsahl, J. Camera, B. Miller and T. Krauss, *J. Am. Chem. Soc.*, 2005, **127**, 7932.

